JACS
JOURNAL OF THE AMERICAN CHEMICAL SOCIETY

Communication

pubs.acs.org/JACS

Designed DNA Crystal Habit Modifiers

Diana Zhang and Paul J. Paukstelis*

Department of Chemistry & Biochemistry and Center for Biomolecular Structure and Organization, University of Maryland, College Park, Maryland 20742, United States

Supporting Information

ABSTRACT: DNA is now one of the most widely used molecules for programmed self-assembly of discrete nanostructures. One of the long-standing goals of the DNA nanotechnology field has been the assembly of periodic, macroscopic 3D DNA crystals for controlled positioning of guest molecules to be used in a variety of applications. With continuing successes in assembling DNA crystals, there is an enhanced need to tailor macroscopic crystal properties—including morphology—to enable their integration into more complex systems. Here we describe the ability to alter and control crystal habits of a 3D DNA crystal formed by self-assembly of a DNA 13-mer. The introduction of "poison" oligonucleotides that specifically disrupt critical noncanonical base-pairing interactions in the crystal lattice leads to predictably modified crystal habits. We demonstrate that the poison oligomers can act as habit modifiers both during the initial crystallization and during growth of shell layers on a crystal macroseed.

DNA's ability to self-assemble into pre-programmed architectures in complex sequence environments has seen it become one of the most widely used molecules for the construction of arbitrary 2D and 3D nanostructures.[1] However, the initial goal of the DNA nanotechnology field was to design periodic 3D lattices, or crystals, with nanoscale features.[2] 3D DNA crystals containing significant solvent space have been envisioned as molecular scaffold frameworks for organizing guest molecules.[3] The development of several types of 3D DNA crystals[4,5] has led to more diverse applications, including uses as macromolecular sieves,[6] for the positioning of small-molecule guests,[7,8] and for the encapsulation of protein enzymes.[9] These applications have demonstrated the potential for DNA crystals to be useful biomaterials with nanoscale structural properties within a macroscale object. A significant portion of the DNA crystal design field has been focused on altering and understanding properties in existing designs[7,10,11] or identifying new DNA motifs to expand structural diversity.[12,13] Inherently, these approaches interrogate the nanoscale properties of the crystals in the form of intermolecular contacts that enable crystallization. Significantly, very little has been done to control macroscopic properties of existing DNA crystals.

One of the fundamental macroscopic properties of crystals is their morphology, or crystal habit. The habit often suggests the underlying periodicity and symmetry of the crystal lattice, and many crystal forms can have more than one habit type. Crystal habit modifiers alter crystal morphology and are commonly used to enhance certain crystal features for particular applications;[14−18] they are important in biomineralization processes.[19,20] Habit modifiers may act in a variety of ways, including thermodynamically by changing surface energies of selective crystal faces, or through kinetic changes that may impact pre-nucleation, nucleation, and growth.[21] A number of models for the mechanism of habit modification for organic and biologically relevant inorganic crystals have been proposed.[22−25] However, in most cases, habit modifiers are found empirically through selective addition during the crystallization process. This leads to limited predictive power as to how the macroscopic crystal properties may change. This is compounded for macromolecular crystals, where there are many more weak intermolecular lattices contacts necessary for maintaining crystal integrity.[26]

We previously characterized a DNA crystal composed of 13 nucleotides, d($G_1G_2A_3C_4A_5G_6C_7T_8G_9G_{10}G_{11}A_{12}G_{13}$), that self-assembles in the presence of divalent cations to form hexagonal unipyramidal crystals (Figure S1A).[5,10] Interactions between 13-mers occur in two regions of base pairing: a B-form duplex between C_4-G_9 of two strands, and a parallel-stranded noncanonical motif between G_1-A_3 and G_{10}-A_{12} of two other strands (Figure S1B). Previous studies suggested that the Crick−Watson pairing between C_4-G_9 occurs only upon the addition of divalent cations, and that the assembly into higher molecular complexes facilitated by the noncanonical pairs also occurred rapidly after Mg^{2+} addition.[10]

The high-resolution crystal structures of the 13-mer and a number of closely related oligonucleotide sequences[10] allowed us to examine lattice features that could be manipulated to potentially alter the macroscopic properties of the crystals. One notable feature was that the hexameric duplex regions were aligned with their helical axes orthogonal to the *c* cell axis (Figure 1). This corresponds to the six-fold symmetry axis in the hexagonal crystal system, leading to the duplexes being layered down this axis while rotated 120° with respect to flanking layers. The ∼2 nm spacing between duplexes within each layer creates a series of solvent channels that run through the crystal in multiple directions (Figure S2). The 5′ nucleotides involved in the noncanonical interactions (G_1-A_3) exit from the duplex helical axis down the *c* axis, while the 3′-most nucleotides (G_{10}-G_{12}) extend out of the helices along the *a* and *b* cell edges (Figure 1). This led us to explore the possibility of disrupting either the 5′- or 3′-most nucleotides to influence crystal growth rates along or orthogonal to the six-

Received: December 5, 2016
Published: January 17, 2017

DOI: 10.1021/jacs.6b12528
J. Am. Chem. Soc. 2017, 139, 1782−1785

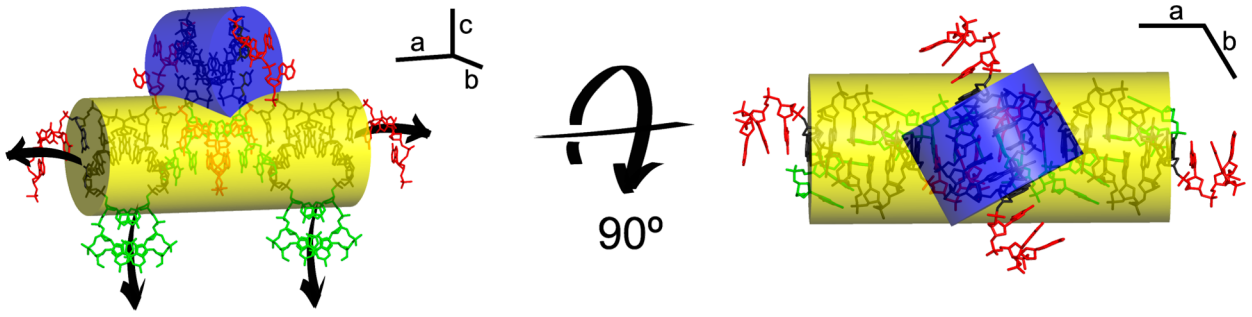

Figure 1. Relative orientations of the duplex segments and noncanonical base pairs in the 13-mer crystal. Duplex regions are overlaid by semitransparent cylinders. The yellow cylinder spans two duplex segments that are coaxially stacked through noncanonical base pairs between 5′ (green) and 3′ (red) nucleotides. The blue cylinder spans a single duplex segment that connects to the two duplexes of the yellow cylinder through its 5′ nucleotides. Arrows in the image on the left represent the direction the terminal nucleotides exit the duplex segments. All duplex helical axes are orthogonal to the *c* cell axis, which positions the 3′ nucleotides along the *a* and *b* cell axes. The 5′ nucleotides exit the duplex segments down the *c* cell axis.

fold symmetry axis. We designed 5′ and 3′ truncated versions of the oligonucleotide that could still form Crick–Watson base pairs with the full-length strands, but would be deficient in forming the noncanonical base pairs (Figure S1A). We reasoned that these truncated oligonucleotides, designated Δ5′ and Δ3′, could selectively "poison" crystal growth and function as crystal habit modifiers.

The poison oligomers were evaluated by adding increasing concentrations of Δ5′ or Δ3′ to crystal drops containing the full-length 13-mer. We observed distinct concentration-dependent crystal habit changes from the starting hexagonal unipyramidal crystal (Figure 2A) with both poison oligomers

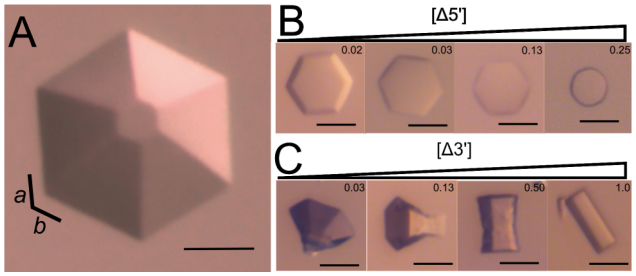

Figure 2. Poison oligomers as crystal habit modifiers. (A) Unipyramidal crystals in the absence of habit modifiers. Relative orientation to unit cell axes is shown. (B) Tabular habit modification in the presence of increasing concentration of Δ5′ poison. (C) Acicular or columnar habit modification with increasing concentration of Δ3′ poison. Scale bars, 70 μm. Relative molar ratios of poison oligomers to 13-mer are shown in the upper right corners.

(Figure 2B,C). Addition of the Δ5′ poison resulted in crystals with preferential growth orthogonal to the *c* cell axis, resulting in a change to a tabular habit (Figure 2B). This transition was dependent on Δ5′ concentration, with the flattening appearing at the lowest concentrations tested. At higher concentrations, crystals appeared as 2D hexagons, and at even higher concentrations crystals did not grow. Addition of Δ3′ also generated a new set of concentration-dependent crystal habits (Figure 2C). At low concentrations, crystals appeared as hexagonal pyramids with slightly elongated points. With increasing Δ3′ concentration, the elongated points showed a discernible hexagonal growth that developed to form "bowtie"-shaped crystals. At the highest concentrations that still gave crystals, the crystals became uniform acicular hexagonal columns. Interestingly, the two poison oligomers showed different concentration dependencies. Habit changes were significantly more sensitive to presence of Δ5′, possibly reflecting a greater affinity between this oligomer and the 13-mer, or different propensities for stable incorporation into the lattice. Crystals grown in the presence of both Δ5′ and Δ3′ favored tabular crystal formation until Δ3′ concentrations were 20-fold excess, at which time they formed crystals with intermediate morphologies that were also dependent on the relative concentration of 13-mer and poison strands (Figure S3). This suggests that the addition of both poison oligomers may allow fine-tuning of the crystal shapes.

Diffraction studies were consistent with the truncated oligomers functioning as habit modifiers and not as more general modifiers of crystal form. Crystals grown in the presence of Δ5′ or Δ3′ had similar unit cell parameters and apparent hexagonal space groups from indexing, while also having decreased diffraction limits (Figure S4). The decreased diffraction limit suggested that the poison strands were incorporated into the crystal lattice, where they would likely cause local structural changes that would decrease lattice order and overall coherent diffraction, while also potentially impacting other physical properties. Electrophoretic analysis of washed, dissolved, and radiolabeled crystals showed low levels of an apparent 9 nt species in crystals grown in either Δ5′ or Δ3′ that was absent in crystals grown without the poison strands (Figure S5). It is unclear why Δ5′ appears truncated by a single nucleotide, though we previously observed that the 3′ terminal guanosine (G_{13}, which is unpaired in the crystal structure) is one of the more labile spots in the crystal. This may be exaggerated in the truncated form.

Detecting the poison oligonucleotides in the crystals suggested that they likely did not exhibit their effects only at crystal nucleation or pre-nucleation, but also during crystal growth. To directly test if the poison strands influenced crystal growth, we performed post-crystallization layering by adding fresh oligonucleotides to pre-formed crystals serving as macroseeds. A small amount of 3′-fluorescein-modified 13-mer (Figure S1A) was included to track the newly grown layer by confocal microscopy. Figure 3 shows a series of *z*-axis slices and 3D reconstructions of hexagonal unipyramidal macroseeds in the presence and absence of poison strands. In the absence of poison strands, a uniform fluorescent layer grew over the pyramidal crystal surface (Figure 3A). In the presence of Δ5′ the fluorescent layer showed preferential growth orthogonal to the six-fold symmetry axis, leading to a significantly enlarged

DOI: 10.1021/jacs.6b12528
J. Am. Chem. Soc. 2017, 139, 1782–1785

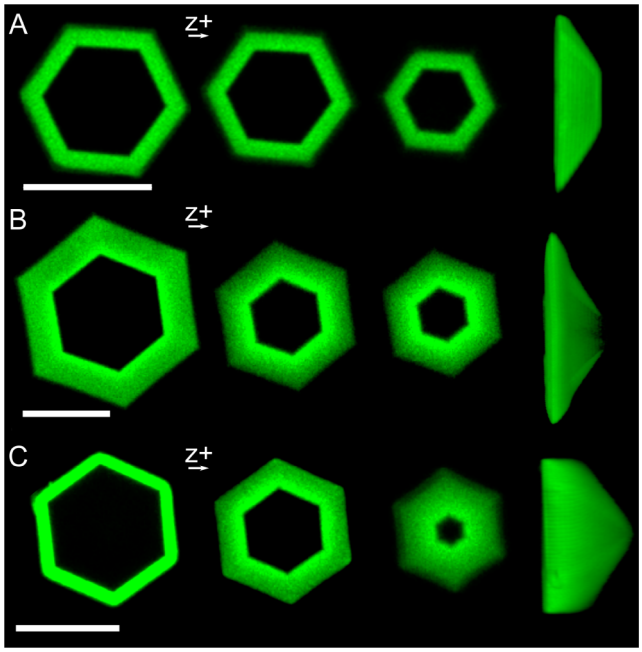

Figure 3. Poison oligmers function as habit modifiers during crystal growth. 13-mer crystal macroseeds were grown in the absence of habit modifiers. The fluorescently modified 13-mer tracks the layer grown on the macroseed. For each panel, three confocal z-stack images down the *c* cell axis are shown, followed by a 3D reconstruction from all z-stack images, shown orthogonal to the *c* cell axis. (A) Macroseed in the absence of poison displays unifom fluorescence accumulation. (B) Shell growth in the presence of Δ5′, leading to a new tabular layer that is significantly thicker along *a*/*b* than that in (A). (C) Layer growth in the presence of Δ3′ is columnar, showing apparent increase in the thickness of the shell layer toward the "top" of the core pyramidal crystal. Changes in crystal morphologies based on layer growth are seen in the 3D reconstructions. Scale bars, 50 μm.

hexagonal base (Figure 3B). In the presence of Δ3′ the crystals showed preferential growth down the six-fold symmetry axis, leading to the growth of a new columnar base region capped by the pyramidal segment as observed in the 3D reconstruction (Figure 3C) and in light microscope images (Figure S6A).

Remarkably, this axis-dependent growth was also observed when tabular or acicular crystals were used as macroseeds (Figure 4). Tabular crystals initially grown in the presence of Δ5′ grew uniform fluorescence layers in the absence of poison and began to grow as unipyramids (Figure 4A). Layer growth in the presence of Δ5′ exacerbated the tabular morphology (Figure 4B), while the presence of Δ3′ led to growth down the *c* axis, resulting in columnar growth from the tabular base (Figure 4C and Figure S6B). Similarly, acicular crystals initially grown in the presence of Δ3′ showed bidirectional layer growth parallel and perpendicular to the *c* axis without poison (Figure 4D), only growth orthogonal to the *c* axis with Δ5′ (Figure 4E), and primarily growth down the *c* axis in the presence of Δ3′ (Figure 4F). Using habit modifiers to control both the shape of the crystal macroseed and the direction of crystal growth on that macroseed opens up the possibility for creating a highly diverse set of crystal morphologies. Significantly, it may be possible to achieve even greater levels of control by including both habit modifiers simultaneously, effectively tuning the growth characteristics.

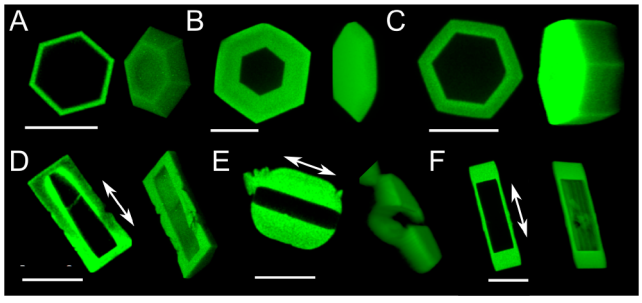

Figure 4. Habit-modified crystals as macroseeds. Each panel contains a confocal image to show layering and a 3D reconstruction to show overall shape: (A) tabular crystals layered without poison strands, (B) in the presence of Δ5′, and (C) in the presence of Δ3′; (D) acicular crystals layered without poison strands, (E) in the presence of Δ5′, and (F) in the presence of Δ3′. Arrows indicate the direction of the *c* cell axis. Scale bars, 50 μm.

Several lines of analysis suggested that the ability for Δ5′ and Δ3′ to function as habit modifiers is dependent on their ability to base-pair with the 13-mer directly, and/or their propensity to be integrated into the growing lattice. First, we confirmed that a related 13-mer sequence that has a nearly identical crystal structure,[10] but with the central G-C base pair of the duplex region converted to a C-G base pair (Figure S1A), showed the same habit modification trends using poison oligonucleotides with sequences complementary to its duplex region (Figure S7A). Second, we observed differences in cross-reactivity when using non-complementary poison strands. Δ3′ showed minimal cross-reactivity in either combination. Though there were impacts on crystal quality, particularly at high poison concentrations (2.5-fold molar excess), there was no clear trend toward the formation of acicular crystals (Figure S7C). Interestingly, the non-complementary Δ5′ poisons did show a trend toward tabular crystals (Figure S7B), though requiring higher concentrations for the effect to be visible relative to the complementary versions. This and the previously noted differences in concentration dependencies of Δ5′ and Δ3′ are most readily explained by their ability to integrate into the growing lattice. Because the duplex region is self-complementary, the poison strands can base-pair with themselves (homopaired) or base-pair with the 13-mer strands (heteropaired). In the case of Δ3′, it is unlikely that homopaired poison strands could be stably integrated into the lattice, as the 3′-most residues are necessary for coaxial stacking of duplexes (Figure S1B). Thus, the higher concentrations are necessary to achieve sufficient concentrations of heteropaired duplex to observe the habit modification effects. Alternatively, homopaired and heteropaired Δ5′ species likely could both be incorporated between duplex regions, meaning lower concentrations would be required to observe habit modification. This is also consistent with the observation that non-complementary Δ5′ poison strands can induce tabular habit modification, as they could be incorporated in the homopaired form.

Here, we have presented an approach to altering the macroscopic properties of a DNA crystal using designed oligonucleotide habit modifiers. The change in crystal habits to a tabular form in the presence of Δ5′ and to an acicular form in the presence of Δ3′ is fully consistent with the relative positions of the 5′ and 3′ nucleotides with respect to the duplex helical axes. The ability to control macroscopic crystal properties, including morphology, provides an important step toward integrated control across scales: the construction of macroscopic objects of controllable shapes and exploitable

DOI: 10.1021/jacs.6b12528
J. Am. Chem. Soc. 2017, 139, 1782−1785

nanoscale features, such as the solvent channels in these crystals. The ability to control shape allows for tunable crystal properties. For example, apparent mass transport effects were observed when DNA crystals containing proteins enzymes were incubated with substrate molecules.[9] By altering crystal shape, it may be possible to control crystal permeability and diffusion through the crystal by selectively adjusting crystal habits to generate solvent channels with different aspect ratios. This demonstration provides a new branch of work in DNA crystal design through the ability to alter both nanoscale and macroscale crystal properties. It is likely that other DNA crystal systems would be susceptible to habit modification using similar techniques. However, the relative orientation of DNA lattice contacts and crystal axes may require more involved design features than the simple truncations used here.

■ ASSOCIATED CONTENT

Supporting Information

The Supporting Information is available free of charge on the ACS Publications website at DOI: 10.1021/jacs.6b12528.

Methods section and Figures S1−S7 PDF)

■ AUTHOR INFORMATION

Corresponding Author

*paukstel@umd.edu

ORCID

Paul J. Paukstelis: 0000-0001-8536-4361

Notes

The authors declare no competing financial interest.

■ ACKNOWLEDGMENTS

The authors acknowledge funding from the National Science Foundation (NSF) through a CAREER award (DMR1149665) to P.J.P.

■ REFERENCES

(1) Jones, M. R.; Seeman, N. C.; Mirkin, C. A. *Science* **2015**, *347* (6224), 1260901.
(2) Paukstelis, P. J.; Seeman, N. C. *Crystals* **2016**, *6* (8), 97.
(3) Seeman, N. C. *J. Theor. Biol.* **1982**, *99* (2), 237.
(4) Liu, D.; Wang, M.; Deng, Z.; Walulu, R.; Mao, C. *J. Am. Chem. Soc.* **2004**, *126* (8), 2324.
(5) Paukstelis, P. J.; Nowakowski, J.; Birktoft, J. J.; Seeman, N. C. *Chem. Biol.* **2004**, *11* (8), 1119.
(6) Paukstelis, P. J. *J. Am. Chem. Soc.* **2006**, *128* (21), 6794.
(7) Wang, T.; Sha, R.; Birktoft, J.; Zheng, J.; Mao, C.; Seeman, N. C. *J. Am. Chem. Soc.* **2010**, *132* (44), 15471.
(8) Melinger, J. S.; Sha, R.; Mao, C.; Seeman, N. C.; Ancona, M. G. *J. Phys. Chem. B* **2016**, *120* (48), 12287.
(9) Geng, C.; Paukstelis, P. J. *J. Am. Chem. Soc.* **2014**, *136* (22), 7817.
(10) Saoji, M.; Zhang, D.; Paukstelis, P. J. *Biopolymers* **2015**, *103* (11), 618.
(11) Stahl, E.; Praetorius, F.; de Oliveira Mann, C. C.; Hopfner, K.-P.; Dietz, H. *ACS Nano* **2016**, *10* (10), 9156.
(12) Muser, S. E.; Paukstelis, P. J. *J. Am. Chem. Soc.* **2012**, *134* (30), 12557.
(13) Tripathi, S.; Paukstelis, P. J. *ChemBioChem* **2016**, *17*, 1177.
(14) El-Shall, H.; Abdel-Aal, E. A.; Moudgil, B. M. *Sep. Sci. Technol.* **2000**, *35* (3), 395.
(15) Titiz-Sargut, S.; Sayan, P.; Avcı, B. *Cryst. Res. Technol.* **2007**, *42* (2), 119.
(16) Fang, X.-L.; Chen, C.; Jin, M.-S.; Kuang, Q.; Xie, Z.-X.; Xie, S.-Y.; Huang, R.-B.; Zheng, L.-S. *J. Mater. Chem.* **2009**, *19* (34), 6154.
(17) Lee, J. Y.; Hong, B. H.; Kim, W. Y.; Min, S. K.; Kim, Y.; Jouravlev, M. V.; Bose, R.; Kim, K. S.; Hwang, I.-C.; Kaufman, L. J.; Wong, C. W.; Kim, P.; Kim, K. S. *Nature* **2009**, *460* (7254), 498.
(18) Mahal, A.; Tandon, L.; Khullar, P.; Ahluwalia, G. K.; Bakshi, M. S. *ACS Sustainable Chem. Eng.* **2016**, *5* (1), 119.
(19) Ndao, M.; Keene, E.; Amos, F. F.; Rewari, G.; Ponce, C. B.; Estroff, L.; Evans, J. S. *Biomacromolecules* **2010**, *11* (10), 2539.
(20) Nancollas, G. H.; Tang, R.; Phipps, R. J.; Henneman, Z.; Gulde, S.; Wu, W.; Mangood, A.; Russell, R. G. G.; Ebetino, F. H. *Bone* **2006**, *38* (5), 617.
(21) Xu, A.-W.; Ma, Y.; Cölfen, H. *J. Mater. Chem.* **2007**, *17* (5), 415.
(22) Volkmer, D.; Fricke, M.; Huber, T.; Sewald, N. *Chem. Commun.* **2004**, No. No. 16, 1872.
(23) Sizemore, J. P.; Doherty, M. F. *Cryst. Growth Des.* **2009**, *9* (6), 2637.
(24) Han, G.; Chow, P. S.; Tan, R. B. H. *Cryst. Growth Des.* **2015**, *15* (3), 1082.
(25) Chung, J.; Granja, I.; Taylor, M. G.; Mpourmpakis, G.; Asplin, J. R.; Rimer, J. D. *Nature* **2016**, *536* (7617), 446.
(26) Heijna, M. C. R.; Enckevort, W. J. P. van; Vlieg, E. *Cryst. Growth Des.* **2008**, *8* (1), 270.

DOI: 10.1021/jacs.6b12528
J. Am. Chem. Soc. 2017, 139, 1782−1785